Nonequilibrium statistical mechanical models for cytoskeletal assembly: Towards understanding tensegrity in cells

Tongye Shen and Peter G. Wolynes
Department of Chemistry & Biochemistry and Department of Physics, University of California, San Diego and Center for Theoretical Biological Physics, La Jolla, California 92093-0371, USA
(Received 9 June 2005; published 26 October 2005)

The cytoskeleton is not an equilibrium structure. To develop theoretical tools to investigate such nonequilibrium assemblies, we study a statistical physical model of motorized spherical particles. Though simple, it captures some of the key nonequilibrium features of the cytoskeletal networks. Variational solutions of the many-body master equation for a set of motorized particles accounts for their thermally induced Brownian motion as well as for the motorized kicking of the structural elements. These approximations yield stability limits for crystalline phases and for frozen amorphous structures. The methods allow one to compute the effects of nonequilibrium behavior and adhesion (effective cross-linking) on the mechanical stability of localized phases as a function of density, adhesion strength, and temperature. We find that nonequilibrium noise does not necessarily destabilize mechanically organized structures. The nonequilibrium forces strongly modulate the phase behavior and have comparable effect as the adhesion due to cross-linking. Modeling transitions such as these allows the mechanical properties of cytoskeleton to rapidly and adaptively change. The present model provides a statistical mechanical underpinning for a tensegrity picture of the cytoskeleton.

DOI: 10.1103/PhysRevE.72.041927 PACS number(s): 87.16.−b, 63.70.+h, 05.10.Gg, 05.70.Ln

I. INTRODUCTION

Life presents us with many structures that are driven far from equilibrium. Examples are abundant even at the level of a single cell. Under the pressure of competition, cells must be able to respond quickly yet in a controllable fashion. Cellular dynamics is not based on passive diffusive processes, but instead uses "active" transport and consumes energy sources, e.g., by the hydrolysis of ATP and GTP [1,2]. Nevertheless the dynamics of individual small protein molecules and ligands are seldom far from equilibrium owing to the relative strength of the thermal buffeting inherent at the smaller length scales. Diffusion alone [3] (or with some help from electrostatic steering [4]) should be enough to move small molecules around. However, the thermal forces by themselves become less capable of moving and reorganizing the larger and larger multi-protein assemblies of the cell. At the scale of entire biological cells, structures are not rearranged just by equilibrium thermal forces but require motors and polymerization processes that use and dissipate chemical energy to form and function. It is therefore interesting to study the generic properties of nonequilibrium structure formation [5] and to answer questions such as how does the far-from-equilibrium character of assembly change the physics of cooperative transitions when compared to equilibrium cases?

The cytoskeleton, a major component of all eukaryotic cells, has long been a mysterious substance (protoplasm!) with unusual physical properties such as active movements and the ability to internally rearrange [2]. These properties are arguably near the top of the list of those attributes that define life as we know it. Motivated by trying to understand the nonequilibrium assembly and remodeling of the cell [1,6], we study here a minimal caricature of the cytoskeleton that has some of its most essential features: a model of interacting motorized particles. As a simplified model, it is designed to answer rather fundamental questions when is such an assembly mechanically stable and when is it fluid, and to what extent can the nonequilibrium forces modulate this? The cytoskeleton in different organisms or even during different parts of the cell cycle exhibits quite a rich variety of viscoelastic properties [7–9]. At a minimum, one imagines that the cytoskeleton should exhibit at least one plastic/fluid phase to facilitate the reorganization of the cell and another elastic/solid phase to support the cell shapes and fulfill other mechanical functions.

Unlike an equilibrium system, we cannot use the ergodicity-based partition function approach to study motorized particle assemblies. Instead, we will study steady states by directly solving a many-body master equation for particle locations using variational methods. As in the theory of equilibrium crystals and quenched glasses, we can use the inverse of the mean-square deviation from a set of fiducial sites as an order parameter to indicate this nonequilibrium transition. The transition from a localized phase to a fluid phase can then be recognized by the localized phonon frequency discontinuously dropping to zero with changing environmental parameters such as decreasing the particle density. We construct and solve the self-consistent equations for this order parameter $\tilde{\alpha}$ from dynamical equations.

Originally the word "tensegrity" [tensional integrity, defined as a stable three-dimensional structure consisting of members under tension that are contiguous and members under compression that are not (Oxford Dictionary)] was used in architecture. This word has recently been used to describe many features of the cytoskeleton. An interesting tensegrity-based model for the cytoskeleton maps the microtubules onto the compression component and other biopolymers the tensional components. This model was proposed and its consequences for cytoskeletal behavior have been discussed by

Ingber and co-workers [10,11]. The tensegrity models considered by engineers and mathematicians [12] have a well-defined (and often simple) deterministic structure. For this reason, the concept has not been accepted completely in the field of cellular mechanics. In a more general sense, the most important concept underlying tensegrity is the existence of a prestress of the system due to the antagonistic interactions among the particles [13]. Thus considering that the forces required for such a strained assembly in the cell are generated by nonequilibrium polymerizations and movements of motor proteins, the present model can be viewed as a statistical treatment of such a generalized tensegrity system.

The paper is organized as follows. We present the physics of our model in Sec. II. The variational methods used to solve for the stability limits of this nonequilibrium many-particle system are presented in Sec. III. We analyze the results in Sec. IV and summarize the importance of nonequilibrium forces for cytoskeletal structures in the last section. A brief summary of this approach dealing with the special case of nonadhesive hard-sphere appeared earlier in Ref. [14].

II. MOTOR-PROPELLED PARTICLES

The forces generated by energy consumption in the cell often have two types of mechanisms: they may arise from (1) rigid or semi-flexible fibril polymerization or from (2) deformation of motor proteins. It has been discovered that the self-assembly processes for actin filaments and microtubules are not near-equilibrium processes [15]. The speeds of polymerizations at the two ends of those linear structures are not the same, so we can have a tread-mill-like "perpetual motion" so long as fuel is available. Through delayed hydrolysis of energetic nucleoside triphosphate (NTP), the system consumes energy and generates motions and forces [1]. One celebrated example of such directed motion by assembly is the "comet tail" created by bacteria *Listeria* to push itself through host bodies by polymerizing actin monomers of host cells [16,17]. A second example is provided by the microtubule aster's ability to position itself by polymerizing tubulin dimers [18]. Besides the direct polymerization induced forces, the "walking" of linear motor proteins on these polymers (such as myosins on actin filaments and dyneins on microtubules) also generates force at the cost of the hydrolysis of corresponding NTPs.

It is therefore very interesting to see how the nonequilibrium aspects of fuel consumption can affect the assembly of structures in cells. Inspired by the statistical mechanics of force-generating self-assembly and remodeling of single fibrils by polymerization as well as models of motor proteins, we build a simple model to study the most generic aspects of nonequilibrium mechanical structures. Our almost literally "spherical cow" model is a collection of particles that interact through an isotropic potential, while the motorized part of their motions still may have anisotropy. These spherical particles are energized by intrinsically attached motors. The radial symmetry assumption for the mechanical part of the interactions is terribly oversimplified for real applications of cytoskeleton assembly, but the spherical model is meant to separate those aspects of the complexity due to the far-from-equilibrium effects from other complications coming from geometry [19,20]. The generalization of these results to more complicated geometries seems quite feasible.

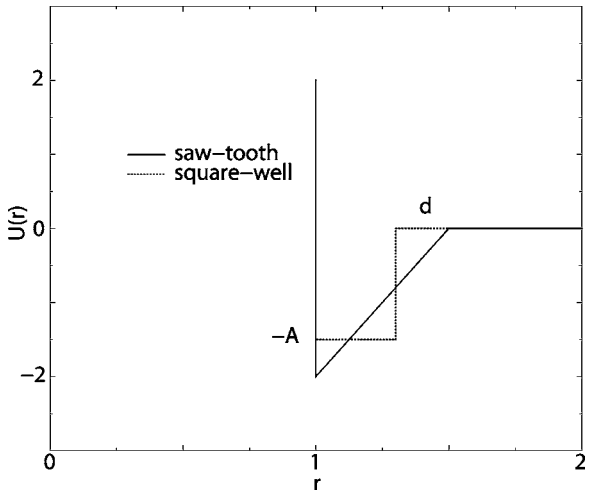

FIG. 1. Adhesive hard sphere potentials $u_{st}(r)$ and $u_{sw}(r)$.

We use a stochastic description of the motions of the particles. This enables us to describe the nonequilibrium noise well. There are three types of forces acting on the particles in motorized particle systems. Apart from (1) the usual (mechanical) interactions $\Sigma u_{ij}(r_{ij})$ between particles, (2) thermal noises and viscosity, there also will be (3) motor propelling forces which obey the rules of the stochastic chemical reactions of single motor molecules.

We model the pairwise interaction $u(r)$ among particles as an adhesive hard-sphere potential. This form is often used when describing biomolecular assembly at equilibrium such as occurs during protein crystallization [21]. Two forms of attractive potential u_{sw} and u_{st} are chosen for our study: the square-well potential $u_{sw}(r) := -A \times \Theta(d-r) + \infty \times \Theta(1-r)$ and the saw-tooth potential $u_{st}(r) := -A[(d-r)/(d-1)] \times \Theta(d-r) + \infty \times \Theta(1-r)$. Both have an energy parameter A to describe the depth of the attraction and a width parameter d to describe the width of the attraction as shown in Fig. 1. The short distance hardcore repulsion part prevents the overlapping of particles. The mid-ranged attractions in this model mimic the effective cross-linking by linker proteins between elements of the cytoskeleton. By using this simplified interaction and using minimal dynamical rules, our model resembles the portrait of the cytoplasm provided by Francis Crick: a "Mother's Work Basket—a jumble of beads and buttons of all shapes and sizes, with pins and threads for good measure, all jostling about and held together by colloidal forces" [22].

The equation of motion for a given motorized particle i is $m_i \ddot{\vec{r}}_i = -\Sigma_{j \neq i} \nabla_i u_{ij} - \gamma \dot{\vec{r}}_i + \vec{\xi}^t(t) + \vec{f}^m(t)$. Here $\vec{r}_i$ is the position of the i th particle and $\vec{\xi}$ and $\vec{f}^m$ are thermal noise and nonequilibrium noise, respectively. The time scales we are interested in are longer than the lifetime of the momentum autocorrelation function (the time scale of typical collisions). By virtue of this clear separation of time scales, we can eliminate fast modes and adopt the overdamped limit of the Langevin

equation: $\vec{r}_i=\beta D\vec{f}_i+\vec{\eta}_i(t)+\vec{v}_i^m$. The thermal noise $\vec{\eta}$ is a Gaussian white noise with the first two moments as $\langle\vec{\eta}_i(t)\rangle=0$ and $\langle\eta_i^\alpha(t)\eta_j^\beta(t')\rangle=2D\delta_{\alpha\beta}\delta_{ij}\delta(t-t')$. Here the systematic force $\vec{f}_i=-\nabla_i U$ is based on the mechanical potential $U(\{\vec{r}\})=\Sigma_{\langle ij\rangle}u(\vec{r}_{ij})$. The motor term $\vec{v}^m(t)=\Sigma_j\vec{\ell}_j\delta(t-t_j)$ gives a time series of shot-noise-like kicks. The noise properties of the motor terms depend on the underlying biochemical mechanism of the motor as we detail below.

To study the possible macroscopic phases of this collection of motorized particles, it is convenient to use the master equation to track the dynamics of the probability distribution function $\Psi(\vec{r}_1,\vec{r}_2,\cdots,\vec{r}_n,t)$ of the particle configurations,

$$[\partial_t-(\hat{L}_{FP}+\hat{L}_{NE})]\Psi(\{\vec{r}\},t)=0 \tag{1}$$

rather than the Langevin description. Here the Fokker-Planck (FP) operator

$$\hat{L}_{FP}\coloneqq D\sum_i\nabla_i\cdot(\nabla_i-\beta\vec{f}_i\cdot) \tag{2}$$

describes the thermal motions. An integral operator $\hat{L}_{NE}$ summarizes the nonequilibrium kicking effect of the motors:

$$\hat{L}_{NE}\Psi(\{\vec{r}\})=\int\Pi_i d\vec{r'}_i\times[K_{\{\vec{r'}\}\to\{\vec{r}\}}\Psi(\{\vec{r'}\})-K_{\{\vec{r}\}\to\{\vec{r'}\}}\Psi(\{\vec{r}\})]. \tag{3}$$

To specify the nature of the chemical noise, we assume the following properties for our simple motors: The motors are firmly built in the particles. They work by consuming chemical energy sources such as ATP. In a single chemical reaction event, the motor makes a power stroke (which induces a discrete conformational change) that moves the particle by a distance of ℓ in the direction $\hat{n}$. Motor kicking can be modeled as a two-step stochastic process: in step I, the energy source binds to the motor, and in step II, the reaction and the resulting conformational change make a power stroke. The rate of the first step depends on the concentration of the energy source while the rate of the second step depends on the coupling between the structural rearrangements and the external forces, $k=k^0\exp\{s\beta[U(\vec{r})-U(\vec{r}+\vec{\ell})]\}$, i.e., motors may slow down when they work against mechanical obstacles.

Note in the case of the cytoskeleton filaments, the kinetics of the "motor" describes the growing and shrinking of the filament which effectively move the center of mass of the "particle." The slowing of the "motor," i.e, the decrease of growth rates of the ends of filaments against walls (thus under tension), has been demonstrated in the case of microtubules [23].

The coefficient s describes the coupling strength between chemical noises and mechanical interaction. The limit that $s\to 1$ will be called a *susceptible* motor and the limit $s\to 0$ an *adamant* motor. We use these names in the sense that an adamant motor is not sensitive to the thermal environment. Each power stroke of such a motor uses and wastes a lot of energy. The difference in the mechanically environmental cost is negligible. On the other hand, the susceptible motor is an energy saving motor since it "rides" with downhill energy and slows down when going uphill. The energy cost is comparable with the part needed to combat the change of the mechanical potential. Since going uphill and downhill may involve two different mechanisms, we specifically use s_u and s_d to label them, i.e., s_u and s_d are not necessarily related. For example, the dynamics of polymerization process has an $s_u>0$ but $s_d=0$. This means growth only slows down with loaded forces [23], but never speeds up. Depending on their detailed biochemistry, motorized particles propelled by real motor proteins could have both s_u and s_d nonzero.

To further simplify, we assume step II (the reaction itself) is the bottle-neck, and therefore the rate of mechanically induced step is only weakly dependent on step I or on the concentration of the source. Thus we presently ignore the complication of noises arising from the binding step, though at low concentration the competition between the particles for fuel may have interesting consequences. We assume the overall statistics of the time-series of kicks is described by a Poisson process with position $\vec{r}$ as $\kappa\exp\{s\beta[u(\vec{r}+\vec{\ell})-u(\vec{r})]\}$.

As for the direction $\hat{n}(t)$, we imagine that it will gradually lose its initial orientation due to the interaction with other particles over a time scale of τ. We study explicitly two extreme cases of motor statistics here, although more general models are possible. For *persistent kicking*, we assume τ is very large compared to the time scale of observation, i.e., each motor always kicks in a predefined direction. There is a special case in which each motor kicks at the same laboratory direction. We term this *polar kicking* (as a distinction between the general *persistent kicking* for which each particle has a preferred direction, but their directions are randomly distributed). For the opposite limit, that where the reorientation τ is very short, we use the term *isotropic kicking*.

III. METHODS: VARIATIONAL APPROACHES

Our strategy to study the stability of nonequilibrium solid phases is as follows: we first construct a set of trial probability distribution functions of particle positions with variable localization parameters under given environmental parameters such as particle density and properties of motorized particles such as kicking strength. We then use nonhermitian variational or square Hermitian variational method to minimize the functional with various trial functions. By changing environmental parameters and tracing the drastic changes of the corresponding optimal solutions, from localized distribution functions to delocalized forms, we can identify the critical parameters for the destabilization transition.

The master equation $\partial_t\Psi=(\hat{L}_{FP}+\hat{L}_{NE})\Psi$ cannot be simply made Hermitian by the canonical transformations of the left and the right states as is commonly done for a usual FP operator. The reason is that the kicking forces from $\hat{L}_{NE}$ cannot be derived from an explicit potential. We need to use either the moment closure method or the square Hermitian method to solve the stochastic many-particle problem.

A. The moment closure (non-Hermitian variational) method

It is unclear whether there is a general variational principle for nonequilibrium systems that can achieve the same

status as the free energy optimizations for equilibrium systems. But it is not unusual to convert a set of dynamical equations to corresponding variational formulations. Still it is a convenient approach, especially for problems with constraints pioneered by Eyink [24]. Since we do not add any constraints, the Eyink procedure gives exactly the same formulation as does the moment closure approach [25].

For convenience, we detail here the calculations for isotropic kicking. We will generalize them to the case of the persistent kicking below. Using the description of the properties of the motor in the previous section, we write the kicking operator's action on states as

$$\hat{L}_{NE}\Psi = \sum_i \kappa_i \int \frac{1}{4\pi} d^2\hat{n} \int d\vec{r'}_i \{ w[U(\ldots,\vec{r'}_i,\ldots) - U(\ldots,\vec{r}_i,\ldots)] \times \delta(\vec{r}_i - \vec{r'}_i - \vec{\ell})\Psi(\{\vec{r'}\}) - w[U(\ldots,\vec{r}_i,\ldots) - U(\ldots,\vec{r'}_i,\ldots)] \times \delta(\vec{r}_i - \vec{r'}_i + \vec{\ell})\Psi(\{\vec{r}\})\}. \quad (4)$$

We assume the time series of the kicks by the motor satisfies Poisson statistics. The rate w is position dependent:

$$w = \exp(s_u \beta \Delta U)\Theta(\Delta U) + \exp(s_d \beta \Delta U)\Theta(-\Delta U). \quad (5)$$

The usual localized Gaussian trial function of the probability distribution function is expressed as

$$\Psi(\{\vec{r}\};\{\vec{R}\}) = \exp\left(-\sum_i \tilde{\alpha}_i(\vec{r}_i - \vec{R}_i)^2\right). \quad (6)$$

Here the positions of particles are $\{\vec{r}\} \equiv \vec{r}_1, \vec{r}_2, \ldots, \vec{r}_N$ and the corresponding $\{\vec{R}\}$ are the fiducial positions about which the particles are localized. The level of delocalization (mean square deviation of the positions around the fiducial positions) is related to $\tilde{\alpha}$ by the relation $\langle(\vec{r}-\vec{R})^2\rangle = 1/(2\tilde{\alpha})$. The potential $U(\{\vec{r}\}) = \Sigma'_{i,j} u(\vec{r}_i - \vec{r}_j)$ is a pairwise summation of interactions having the form $u(\vec{r}) = +\infty$ if $|\vec{r}| < 1$ and 0 or finite values otherwise. However, there is an extra obstacle to overcome for the case of the hardcore potentials. For the operator $\hat{L}_{FP} = D\Sigma_i \nabla_i \cdot (\nabla_i + \beta \nabla_i U(\{\vec{r}\})\cdot)$, the term $\nabla\cdot(\nabla U\cdot)$ will be singular at the hardcore boundary when it operates on the usual localized Gaussian trial function Ψ.

To solve a similar singularity problem appeared in the quantum many-body system of hard spheres, Jastrow proposed [26] a new trial function by adding an extra Boltzmann factor $\exp(-\beta U)$ to the original form. Here we also adopt the Jastrow trial function

$$\Psi(\{\vec{r}\}) = \exp\left(-\sum_i [\xi_i(\vec{r}_i - \vec{R}_i)^2] - \beta U(\{\vec{r}\})\right). \quad (7)$$

One may question this form of the trial function since $\exp(-\beta U)$ itself should be the exact equilibrium solution of a usual Fokker-Planck equation. Two things are different here. One aspect is the nonequilibrium effects. The other is that even for equilibrium cases, we study the localized phase of a many-particle problem which has a symmetry-breaking transition from the fluid phase and therefore its probability distribution function will not be the same, but instead it will be determined by an effective localized trial function. We need to replace $U(\{\vec{r}\})$ with localized forms eventually. With the Jastrow term in the trial function, the singularity is formally canceled out. To simplify the notation, we write for the displacement of the particle off the fiducial site $\vec{q}_i = \vec{r}_i - \vec{R}_i$ below. Since the diffusion term of the FP operator has $D\nabla_i^2\Psi = D\{[2\xi_i\vec{q}_i + \beta\nabla_i U(\{\vec{r}\})]^2 - 6\xi_i - \beta\Delta_i U(\{\vec{r}\})\}\Psi$ and the drift term of the FP has $D\beta\nabla_i\cdot[\nabla_i U(\{\vec{r}\})\Psi(\{\vec{r}\})] = D\beta[-\nabla_i U\cdot(2\xi_i\vec{q}_i + \beta\nabla_i U) + \Delta_i U]\Psi$, we can cancel out terms of $(\nabla_i U)^2$ and $\Delta_i U$ by adding two parts together. This leaves

$$\hat{L}_{FP}\Psi = \sum_i (4D\xi_i^2 q_i^2 - 6D\xi_i + 2\xi_i\beta D\vec{q}_i\cdot\nabla_i U)\Psi. \quad (8)$$

The remaining term involving $(\vec{q}_i\cdot\nabla_i U)\Psi$ can be calculated even for the case of hard-sphere potential. For example, the term $\int \vec{q}_i\cdot\nabla_i U\Psi d^3\vec{q}\Pi_{j\neq i} d^3\vec{r}_j$ can be first rewritten as $-\beta^{-1}C\int\Pi_{j\neq i}d^3\vec{r}_j \exp(-\Sigma_j\xi_j q_j^2)\int e^{-\xi_i q_i^2}\vec{q}_i\cdot\nabla_i \exp(-\beta U)d^3\vec{q}_i$. Then, applying the identity $(\nabla f)\cdot\vec{v} \equiv \nabla\cdot(f\vec{v}) - f(\nabla\cdot\vec{v})$ and assuming that surface integrals go to zero, we have $\int e^{-aq^2}\vec{q}\cdot\nabla\exp[-\beta U(\vec{q})]d^3\vec{q} = -\int\exp[-\beta U(\vec{q})]e^{-aq^2}(3-2aq^2)d^3\vec{q}$. Therefore, $\int\vec{q}_i\cdot(\nabla_i U)\Psi d^3\vec{q}_i\Pi_{j\neq i}^N d^3\vec{r}_j = \int\Pi_{j=1}^N d^3\vec{r}_j\beta^{-1}(3-2\xi_i q_i^2)\Psi$. Using this result, it is easy to confirm the conservation of the probability $\langle 1|\hat{L}_{FP}|\Psi\rangle \equiv 0$. Similarly we can calculate higher order moment operators that are weighted by q_j^n. If $i \neq j$, there is a decoupling for the q_i integrations. Otherwise, for $i=j$, we can use $\nabla\cdot(e^{-aq^2}q^n\vec{q}) = e^{-aq^2}q^n(n+3-2aq^2)$ to proceed.

We also need to evaluate integrations of the form $\int\Pi_i d^3\vec{q}_i Q(q_j)\exp[\Sigma - \xi_i q_i^2 - U(\{\vec{r}\})]$. Here $Q(q_j)$ is a polynomial function of a local one-body displacement operator or other few-body operators. These integrals generally do not have exact solutions. It turns out the integrals we meet here also appear in similar forms in evaluating partition functions of the corresponding equilibrium theory of crystallization [27] or glass transition [28]. We can thus borrow the thermodynamic integration and the cluster expansion method to proceed. For example, in the case of $Q(q_j) \equiv 1$, we rewrite $\int\Pi_i d^3\vec{q}_i \exp[\Sigma - \xi_i q_i^2 - U(\{\vec{r}\})] = C_o\langle e^{-U}\rangle_o$. Here $C_o = \int\Pi_i d^3\vec{q}_i \exp(\Sigma - \xi_i q_i^2) = \Pi_i(\pi/\xi_i)^{3/2}$ and $\langle\cdot\rangle_o$ is the Gaussian average. We approximate $\langle e^{-U}\rangle_o = \langle\Pi_i e^{-u_i}\rangle_o \approx \Pi_i\langle e^{-u_i}\rangle_{x(i)}$. Here $u_i = \Sigma_{j\neq i}\frac{1}{2}u_{ij}$. The bracket $\langle\cdot\rangle_{x(i)}$ indicates the independent average over the distribution of the displacement of the nearest neighbor of index i. As a result, we have $\int\Pi_i d^3\vec{q}_i \exp[\Sigma - \xi_i q_i^2 - U(\{\vec{r}\})] = C_o\Pi_i[(\xi_i + \alpha_i)/\xi_i]^{-3/2}$. Here α_i are the eigenvalues of the Hessian matrix constructed from the effective local potential $(\frac{1}{2})\bar{u}_i$ that has the form $e^{-\bar{u}_i} = \langle e^{-u_i}\rangle_{x(i)}$. Thus we rewrite the effective local potential $\bar{u}_i = \xi_i q_i^2 + \Sigma_{j\in n.n.} v^e(|\vec{R}_i - \vec{R}_j|)$. Here v^e is the pairwise Mayer f-bond potential. We denote the total effective spring constant $\tilde{\alpha} := \alpha + \xi$. Here α comes from the effective interaction with the neighboring particles by the Mayer f-bonds and ξ comes from nonequilibrium kicking. Similarly, for the higher moments $Q(q_j) = q_j^n$, we have $\int(\Pi_i d^3\vec{q}_i)q_j^n \exp(\Sigma - \xi_i q_i^2 - U(\{\vec{r}\})) = C_o\tilde{\alpha}_j^{-n/2}[\Gamma((3+n)/2)/\Gamma(3/2)]\Pi_i(\tilde{\alpha}_i/a_i)^{-3/2}$.

To evaluate $\langle q_j^2|\hat{L}_{FP}|\Psi\rangle$, we assume spatially uniform $\xi_i=\xi$ and $\tilde{\alpha}_i=\tilde{\alpha}$. We also ignore the common normalization factor $\langle 1|\Psi\rangle=C_o(\tilde{\alpha}/a)^{-3N/2}$ for now. The aforementioned operator $\hat{L}_{FP}$ has total three parts. For the first part, since $\langle q_j^2|4D\xi^2 q_i^2|\Psi\rangle=9D\xi^2(\frac{3}{2})^2\tilde{\alpha}^{-2}$ if $i\neq j$ and $15D(\xi/\tilde{\alpha})^2$ if $i=j$, we have $\langle q_j^2|\Sigma_i 4D\xi^2 q_i^2|\Psi\rangle=D(\xi/\tilde{\alpha})^2[9(N-1)+15]$. The second and third part are $\langle q_j^2|-\Sigma_i 6D\xi|\Psi\rangle$ and $\langle q_j^2|\Sigma_i 2\xi\beta D\vec{q}_i\cdot\nabla_i U|\Psi\rangle$. All together we thus have $\langle q_j^2|\hat{L}_{FP}|\Psi\rangle=6D(\xi/\tilde{\alpha})$. By the arguments of moment closure, we have

$$\partial_t\langle q_j^2\rangle=\langle q_j^2|\hat{L}|\Psi\rangle \tag{9}$$

Thus with a pure FP system and under equilibrium condition, we have $\partial_t\langle q_j^2\rangle=0=\langle q_j^2|\hat{L}_{FP}|\Psi\rangle=6D(\xi/\tilde{\alpha})$. Therefore $\xi=0$ and $\tilde{\alpha}=\alpha$ as we expected.

Now with the kicking operator $\hat{L}_{NE}=\Sigma_i\hat{L}_{NE}^{(i)}$ added in, we have $\tilde{\alpha}\neq\alpha$. For $i\neq j$, $\langle q_j^2|\hat{L}_{NE}^{(i)}\Psi\rangle=\kappa\langle 1|\Psi\rangle(\frac{3}{2})\tilde{\alpha}^{-1}(\pi/\tilde{\alpha})^{-3/2}(J_0-J_0')=0$ and for $i=j$, $\langle q_i^2|\hat{L}_{NE}^{(i)}\Psi\rangle=\kappa\langle 1|\Psi\rangle(\pi/\tilde{\alpha})^{-3/2}(J_2-J_2')$. Here $J_n=\int d^3\vec{q}\vec{q}^n\langle\times e^{-\tilde{\alpha}(\vec{q}-\vec{\ell})^2}e^{f(-2\alpha\vec{\ell}\cdot\vec{q}+\alpha\ell^2)}\rangle_{\vec{\ell}}$ and $J_n'=\int d^3\vec{q}\vec{q}^n e^{-\tilde{\alpha}\vec{q}^2}\langle e^{f(-2\alpha\vec{\ell}\cdot\vec{q}-\alpha\ell^2)}\rangle_{\vec{\ell}}$. For convenience, we define $f(x)=\Theta(x)s_u x+\Theta(-x)s_d x$. With the transform $\vec{q}\to\vec{q}+\vec{\ell}$ of J', we can combine two terms to a simpler form $I_n:=J_n-J_n'=\int d^3\vec{q}[(\vec{q}+\vec{\ell})^n-\vec{q}^n]e^{-\tilde{\alpha}\vec{q}^2}\langle e^{f(-2\alpha\vec{\ell}\cdot\vec{q}-\alpha\ell^2)}\rangle_{\vec{\ell}}$.

For isotropic kicking, since we need to average over directions of $\vec{\ell}$ and integrate over $\vec{q}$, it is easy to use a spherical coordinate that has $\vec{\ell}$ parallel to the polar axis. The polar angle θ reflects the angle between the direction of $\vec{\ell}$ and the potential gradient. It detects whether the particle is going uphill or downhill. By setting $x:=-\cos\theta$, we use s_u for going upward, against the potential for the range $x\in(-1,\ell/2q)$ and use s_d for going downhill for the range $x\in(\ell/2q,1)$, since the critical angle $\theta_c=\arccos x_c$ satisfies the geometric criterion $-2\alpha\ell q\cos\theta_c-\alpha\ell^2=0$. We still retain azimuthal symmetry. We thus can write

$$\begin{aligned}I_2&=\int_0^\infty dq 2\pi q^2 e^{-\tilde{\alpha}q^2}\left[\int_{-1}^{\ell/2q}dx(-2q\ell x+\ell^2)e^{2s_u x\alpha q\ell-s_u\alpha\ell^2}\right.\\&\left.+\int_{\ell/2q}^{1}dx(-2q\ell x+\ell^2)e^{2s_d x\alpha q\ell-s_d\alpha\ell^2}\right]\\&=\int dq 2\pi q^2 e^{-\tilde{\alpha}q^2}\left[\frac{1-e^{-\alpha\ell^2 s_u-2\alpha\ell q s_u}(1+s_u\alpha\ell^2+2\alpha\ell q s_u)}{2\alpha^2\ell q s_u^2}\right.\\&\left.+\frac{e^{-\alpha\ell^2 s_d+2\alpha\ell q s_d}(1+s_d\alpha\ell^2-2\alpha\ell q s_d)-1}{2\alpha^2\ell q {s_d}^2}\right].\end{aligned} \tag{10}$$

If $s_u=0$ (or $s_d=0$), the corresponding part in the brackets [ ] of the above equation will be reduced to $\ell^2+\ell^3/4q+\ell q$ (or $\ell^2-\ell^3/4q-\ell q$). Finally, based on Eq. (7), we derive the equation of the final localization strength $\tilde{\alpha}$ in terms of the mechanical supports of the neighbors with the mechanical strength α:

$$6D\frac{\tilde{\alpha}-\alpha(\tilde{\alpha})}{\tilde{\alpha}}+\kappa I_2(\tilde{\alpha},\alpha)\left(\frac{\pi}{\tilde{\alpha}}\right)^{-3/2}=0. \tag{11}$$

The equation $\alpha=\alpha(\tilde{\alpha})$ self-consistently determines the mechanical interaction feedback given the value of the neighbor's $\tilde{\alpha}$. The integral I_n can be ultimately rewritten in forms of hypergeometric functions of type I. For $n=2$, we have explicitly

$$\begin{aligned}I_2(\tilde{\alpha},\alpha)=&\frac{\pi}{2\tilde{\alpha}\alpha^2\ell s_u^2}-\frac{\pi}{2\tilde{\alpha}\alpha^2\ell s_u^2}(1+s_u\alpha\ell^2)e^{-s_u\alpha\ell^2}\left\{1-e^{(\alpha\ell s_u)^2/\tilde{\alpha}}\sqrt{\frac{\pi}{\tilde{\alpha}}}\alpha s_u\ell\left[1-\mathrm{erf}\left(\ell s_u\frac{\alpha}{\sqrt{\tilde{\alpha}}}\right)\right]\right\}\\&-\frac{\pi}{2s_u}\tilde{\alpha}^{-5/2}e^{-s_u\alpha\ell^2}\left\{\sqrt{\pi}\left(\frac{\tilde{\alpha}}{\alpha}+2\alpha\ell^2 s_u^2\right)\left[1-\mathrm{erf}\left(\frac{\alpha}{\sqrt{\tilde{\alpha}}}\ell s_u\right)\right]e^{(\alpha\ell s_u)^2/\tilde{\alpha}}-2\ell s_u\frac{\alpha}{\sqrt{\tilde{\alpha}}}\right\}\\&+\frac{\pi}{2\tilde{\alpha}\alpha^2\ell {s_d}^2}(1+s_d\alpha\ell^2)e^{-s_d\alpha\ell^2}\left\{1+e^{-(\alpha\ell s_d)^2/\tilde{\alpha}}\sqrt{\frac{\pi}{\tilde{\alpha}}}\alpha s_d\ell\left[1+\mathrm{erf}\left(\ell s_d\frac{\alpha}{\sqrt{\tilde{\alpha}}}\right)\right]\right\}\\&-\frac{\pi}{2s_d}\tilde{\alpha}^{-5/2}e^{-s_d\alpha\ell^2}\left\{\sqrt{\pi}\left(\frac{\tilde{\alpha}}{\alpha}+2\alpha\ell^2 {s_d}^2\right)\left[1+\mathrm{erf}\left(\frac{\alpha}{\sqrt{\tilde{\alpha}}}\ell s_d\right)\right]e^{(\alpha\ell s_d)^2/\tilde{\alpha}}+2\ell s_d\frac{\alpha}{\sqrt{\tilde{\alpha}}}\right\}-\frac{\pi}{2\tilde{\alpha}\alpha^2\ell {s_d}^2}.\end{aligned} \tag{12}$$

For the case of $s_u=0$ (or $s_d=0$) the first (or last) two lines of the above equation will be given as $(4+2\sqrt{\tilde{\alpha}\pi}\ell+\tilde{\alpha}\ell^2)\ell\pi/4\tilde{\alpha}^2$ (or $-(4-2\sqrt{\tilde{\alpha}\pi}\ell+\tilde{\alpha}\ell^2)\ell\pi/4\tilde{\alpha}^2$). In the special case $s_u=s_d=0$, we have $\alpha/\tilde{\alpha}=1+\kappa\ell^2/6D$. This agrees with the conclusion of the small ℓ limit (by Taylor expansions) solutions of the square Hermitian method discussed in the next subsection.

B. The square Hermitian variational method

Apart from the above moment closure method, one can always generally square a non-Hermitian operator $\hat{L}$ to form

a new operator $\hat{L}^{\dagger}\hat{L}$ thereby making it Hermitian and therefore allowing now a conventional optimization over trial functions to determine the steady states (see, for example, p. 158 of [29]). This procedure is quite difficult algebraically for a complicated many-particle non-Hermitian operator. Here instead we use it for a single-particle approach. First we solve and thus obtain the total effective localization parameter $\tilde{\alpha}$ of one tagged particle under one-particle operator $\hat{l}$ with a *given* mechanical feedback from neighbors with localized parameter α, i.e., we define $\partial_t = \hat{l} = \hat{l}_{FP} + \hat{l}_{NE}$. Here $\hat{l}_{FP} = D\nabla^2 + D\nabla\cdot(\beta D \nabla u_{mec}\cdot)$ and $\beta u_{mec}(r) = \alpha r^2$. The kicking operator acts on states as follows:

$$\hat{l}_{NE}\phi(\vec{r}) = \kappa\psi(\vec{r}-\vec{\ell})e^{\varepsilon(\vec{r}-\vec{\ell})} - \kappa\psi(\vec{r})e^{\varepsilon(\vec{r})} \tag{13}$$

for persistent kicking cases, and

$$\hat{l}_{NE}\phi(\vec{r}) = \frac{\kappa}{4\pi}\int d\hat{n}[\psi(\vec{r}-\hat{n}\ell)e^{\varepsilon(\vec{r}-\hat{n}\ell)} - \psi(\vec{r})e^{\varepsilon(\vec{r})}] \tag{14}$$

for isotropic kicking cases. Here $\varepsilon(\vec{r}) = s\beta\vec{\ell}\cdot(-\nabla u_{mec})$ and s is s_u or s_d depending on whether the kicks are uphill or downhill.

The first step is to use the square Hermitian functional minimization over appropriate trial functions. Then we solve for the mechanical feedback strength α with total localization parameter $\tilde{\alpha}$ obtained from the first step of the calculation. We thus update the values of α and recalculate step one. These two steps are iterated till the α and $\tilde{\alpha}$ convergences.

The single-particle trial function that we try to minimize has a Gaussian form $\psi^G(\vec{r};\alpha) = \exp(-\bar{\tilde{\alpha}}:\vec{r}\vec{r} + \vec{r}\cdot\vec{b})$. Here the off-center displacement of the fiducial sites $\vec{b}$ is parallel to $\hat{n}$ for the persistent kicking and is set to zero for the isotropic kicking. Solving the target equation $\hat{l}\psi^*(\vec{r}) = \partial_t\psi^*(\vec{r}) \equiv 0$ can be posed as a minimization problem with the score function $I[\alpha] = \int d\vec{r}[\partial_t\psi^G(\vec{r};\alpha)]^2$, since the square Hermitianized operator gives $\langle\phi, \hat{l}^{\dagger}\hat{l}\phi\rangle = \int(\hat{l}\phi)^2 d\vec{r}$. Generally the optimal tensor $\bar{\tilde{\alpha}}$ is no longer isotropic, so the final value is set as the harmonic mean, i.e., $\alpha \equiv 3(\alpha_1^{-1} + \alpha_2^{-1} + \alpha_3^{-1})^{-1}$, where α_i are the eigenvalues of $\bar{\tilde{\alpha}}$.

The minimization of the above score functions was carried out numerically. We now take a detour to discuss the 1D results at the limit of small ℓ with Taylor expansion for the specific case under the condition $s_u = s_p = 0$ and persistent kicking. Though this is not as general an approach as the numerical calculations by variation, it gives some physical insights. In the simple 1D case, we have

$$\begin{aligned}\hat{l}\psi(x) &= \partial_t\psi(x)\\ &= D\nabla^2\psi(x) - \nabla\cdot[\beta D(-\partial_x u(x))\psi(x)]\\ &\quad + \kappa\psi(x-\ell) - \kappa\psi(x)\end{aligned} \tag{15}$$

with $u(x) = \beta^{-1}\alpha x^2$.

Up to the second order in ℓ, we have

$$\begin{aligned}\partial_t\psi(x,t) &= D\psi'' - \partial_x[\beta D(-\partial_x u(x))\psi]\\ &\quad - \kappa\ell\psi' + (1/2)\kappa\psi''\ell^2 + O(\ell^3) = 0.\end{aligned} \tag{16}$$

Thus for steady-state solutions, we can construct the effective potential $\bar{u}(x) = \beta^{-1}\tilde{\alpha}(x-b)^2$. Here $\tilde{\alpha} = \alpha/(1 + \kappa\ell^2/2D)$ and mean shift $b = \kappa\ell/(2\alpha D)$. The final localization parameter $\tilde{\alpha}$ is thus seen in such cases to be smaller than the mechanical feedback α, i.e., kicking mobilize the particles and destabilize the structure. Note this is always the case for $s_u = s_d = 0$. However, more generally it turns out we can have $\tilde{\alpha} > \alpha$ for $s_u + s_p > 1$ as we shall demonstrate below.

C. Mechanical feedback and self-consistent phonon theory

Though the two methods listed give different approximate solutions to the non-Hermitian master equation, they both require calculating the mechanical response $\alpha = \alpha(\tilde{\alpha})$. This is essential for the correct description of interactions between particles and is closely related to the self-consistent phonon (s.c.p.) theory of equilibrium crystals and glasses. The self-consistent phonon theory was initially developed to study the anharmonic effects of crystals [27,30,31]. Viewed from the standpoint of thermal stability in an equilibrium system, a particular atom's thermal fluctuation around its fiducial position is the *same* type of fluctuation as its neighbors which is used to average the interactions. [27]. This idea was further extended to hard-sphere amorphous systems but the summation over discrete crystalline neighboring atoms is replaced by integration of a continuous radial distribution function [28]. Recently, this approach was used for the network glasses, too [32].

There are several ways we can calculate the phonon frequency (or the mechanical response α). The crude bare potential phonon approach exchanges the order of averaging and exponentiation operations. On the other hand, Fixman's approach to the equilibrium self-consistent phonon method is a more robust and systematic method that employs an expansion in Hermitian functions. We follow Fixman's s.c.p. approach that averages the Mayer f-bond potential instead of the bare potential [27,28]. The effective potential from the Mayer f-bond $v^e(R)$ is the logarithm of the mean of the exponentiation of the bare interaction $u(R)$ between a tagged particle (fixed at center) and a neighboring particle which is fluctuating with variance $\sim\tilde{\alpha}^{-1}$ around its mean position $\vec{R}$. More succinctly, $\exp[-v^e(R)] = \langle\exp[-u(r)]\rangle_{R,\tilde{\alpha}}$. For a pure hard-sphere potential, this recipe gives

$$\begin{aligned}\beta v^e_{hs}(R) = \ln\Bigg(1 + \frac{1}{2}\,\mathrm{erf}[(R-1)\sqrt{\tilde{\alpha}}] - \frac{1}{2}\,\mathrm{erf}[(R+1)\sqrt{\tilde{\alpha}}]\\ + \frac{(\tilde{\alpha}\pi)^{-1/2}}{2R}[e^{-\tilde{\alpha}(R-1)^2} - e^{-\tilde{\alpha}(R+1)^2}]\Bigg).\end{aligned} \tag{17}$$

We can also use the Mayer f-bonds for adhesive potentials to obtain similar equations. With our definitions of u_{st} and u_{sw} we can again express the final results using the error function $\mathrm{erf}(x)$.

The information about the bare interactions $u(r)$ (which may be singular) is thus contained in the smoother Mayer f-bonds. The structures of the particle assembly need only be specified in terms of the neighboring particle distributions, i.e., the fiducial site arrangements. Below we study localized phases of both ordered crystalline and randomly packed glassy structures. The total effective interactions are the sum of Mayer f-bonds of a central particle with all of its neighbors. Once we have the final potential V, the quadratic term of the expansion makes the story self-consistent and gives back the effective spring constant of the mechanical feedback α.

For calculations on the fcc lattice, we use the 12 first shell neighbor (n.n.) particles to construct $V^{cr}(\vec{r}) = \Sigma_{R_j \in n.n.} v^e(\vec{r} - \vec{R}_j)$. We set the resulting $\alpha^{cr} \equiv 3(\alpha_1^{-1} + \alpha_2^{-1} + \alpha_3^{-1})^{-1}$; here $2 \times \alpha_i$ comes from the eigenvalues of the Hessian matrix J which is defined by $J_{ij} = \partial_{x_i} \partial_{x_j} V^{cr}(\vec{r})$. For the fcc lattice, we generally have $\alpha_1 = \alpha_2 = \alpha_3$.

For the randomly packed solid modeling the glass, we average over an environment in such a way that the previous summation over discrete sites in the crystal is replaced by an integration over a pair distribution. While such distributions can be found from a simulation, the fiducial site distributions can be also approximated as the radial distribution functions of hard-sphere liquids [28]. We have

$$\alpha^{th,g} = (\beta n/6) \int_{1st.sh.} g(R) Tr \nabla \nabla V^s(\vec{R}) d\vec{R}$$
$$= \frac{1}{2} \int_1^{r^*} dr g(r) 4\pi n r^2 \left(\frac{V^{s\prime}(r)}{r} \langle \sin^2 \theta \rangle + V^{s\prime\prime}(r) \langle \cos^2 \theta \rangle \right)$$
$$= \int_1^{r^*} dr g(r) 4\pi n r^2 \left[\left(\frac{1}{3} \right) \frac{V^{s\prime}(r)}{r} + \left(\frac{1}{6} \right) V^{s\prime\prime}(r) \right]. \quad (18)$$

Here r^* is the upper boundary of the effective first shell cutoff which is at the position that function $r^2 g(r)$ reaches its first minimum.

The radial distribution function $g(r)$ is the important input for the glass calculations. For the case of the pure hard-sphere potential, we use the Verlet and Weis's corrected radial distribution function [33] of simple hard-sphere fluid. Generally for other potentials $u(r)$, the effective hard sphere $g(r)$ can still be used as the reference system with an effective radius determined from the full interaction $u(r)$ and $k_B T$ [34]. Here for our adhesive potentials u_{sw} and u_{st}, we have $r_{eff} = 1$, i.e., they have the same hard-core radius. We express the effects of adhesion through only changing the strength of Mayer f-bond due to the difference between $u_{sw/st}$ and u_{hs}. Thus we do not alter the underlying structural dependence.

There is a complication for the cases of persistent kicking when we evaluate the mechanical feedback due to the distortions of the fiducial positions, i.e., we must consider the effects of the off-center shift parameter b on α which distorts the usual static jammed structures. If the directions of the persistently kicking motors are not inhomogeneously distributed, we can model this effect by replacing each initial position with a dispersed kernel: for the crystalline case, this means the neighbor's fiducial position at $\vec{R}_j$ will be further replaced by an average over positions $\vec{R}_j + b\hat{n}$ with $\hat{n}$ as an arbitrary unit direction. Similarly, the radial distribution function of the glass case will change from the initial $g_0(\vec{r})$ to $g_b(\vec{r}) = \int g_0(\vec{r}\,') (1/4\pi b^2) \delta(|\vec{r}\,' - \vec{r}| - b) d\vec{r}\,'$.

This procedure will blur the sharp boundary of $g_0(r)$ at $r = 1$. For all the potentials with hardcore $r = 1$ (as we use throughout the present paper), we need to enforce the condition $g(r) = 0$ for $r < 1$. We thus integrate the region of $r \in [0, 1]$ and renormalize them to the region $1 < r < r^\star$, i.e., $\tilde{g}_b(r) = g_b(r) \Theta(r-1) \times (1+w)$ where $w \equiv [\int_0^1 r^2 g(r) dr] / [\int_1^{r^\star} r^2 g(r) dr]$.

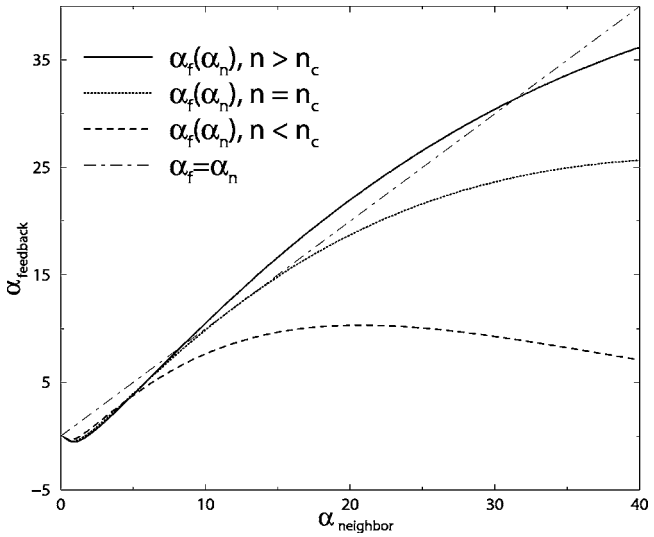

FIG. 2. The illustration of the onset of localized phase with nonzero order parameters by increasing density. The self-consistent equation $f(\alpha; n) = \alpha$ only has zero solution at low density. For $n > n_c$, it has two nonzero fixed points. The stable solution is the one with the derivative less than one, i.e., the one with larger value of α of the two.

IV. RESULTS: THE STABILITY OF THE FAR-FROM-EQUILIBRIUM SOLIDS

A. Effects of adhesiveness

First let us review the results for the systems considered at equilibrium. When we turn off the kicking terms, both variational methods detailed in the method section give the same results, i.e., for equilibrium cases when $\hat{L}_{NE} = 0$, both methods return to the self-consistent phonon method. For pure hard-sphere cases, we recovered the same numerical results of calculations as previous researchers [28]. The stability limit is $n = 0.8685$ for the fcc lattice and $n = 0.94$ for the glass by the s.c.p. method (with the first order cutoff). The corresponding phonon frequency is $\alpha = 12.422$ for fcc and 19.4 for glass.

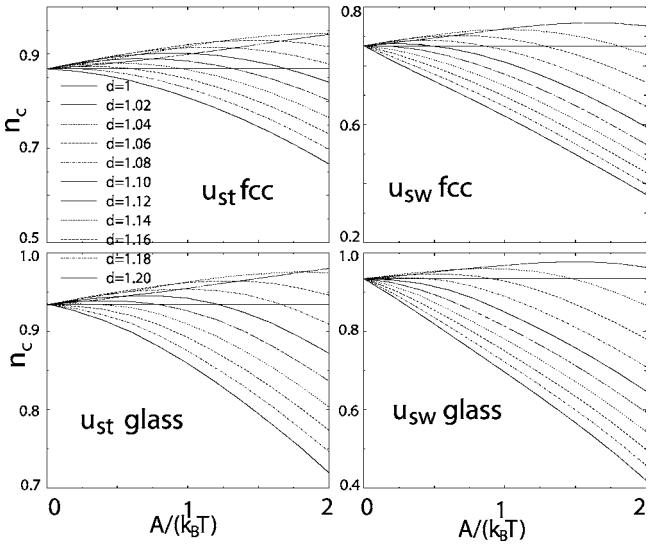

FIG. 3. Effects of $u(r;A,d)$ on critical density $n_c(A,d)$ without motorization for fcc lattice and glass.

We use the fcc case to illustrate the general strategy of finding critical density and phonon frequency which we employ for the other cases. This is shown in Fig. 2. We see that it is relatively more difficult to obtain highly accurate values for critical frequency α than to simply find the critical density n, since at the critical values of self-consistent curve $f(\alpha;n_c)$ is nearly tangential to the diagonal line $y=x$. These two lines are almost parallel for a range of values of α. Thus it is easy to judge whether there is a crossover (to pin down n), but rather more difficult to pin down the α where the crossover happens numerically. Generally it is also more difficult to achieve high accuracy for the glass cases than it is for crystal cases since the final integrations are somewhat prone to numerical inaccuracies.

We are not aware of any reported calculations of adhesive hard-sphere potentials using the self-consistent phonon even for equilibrium solids. There are some calculations for adhesive hard spheres by other methods focusing on the liquid side of the transition such as mode coupling [35]. We first therefore examine the effect of adhesion on equilibrium hard-sphere systems with our method.

We show in Fig. 3 the critical densities of adhesive spheres as functions of the dimensionless parameter characterizing the strength of the adhesion, the ratio of the adhesive energy over the thermal energy A/k_BT. We do this for a given set of width parameter d for the saw-tooth and the square-well potentials and for the equilibrium fcc lattice and the randomly packed structures. At small values of d, we observe that there is first a liquefaction, then a reentrant crystal transition or reentrant glass transition with increasing A/k_BT. This reentrant transition is somewhat counterintuitive. Some researchers who found this result via mode coupling believe it to be caused by the small attractions helping the system to form small clusters, thereby "opening up holes" and making the system more fluid-like [36]. Overall for large d and/or A the present treatment yields a lower

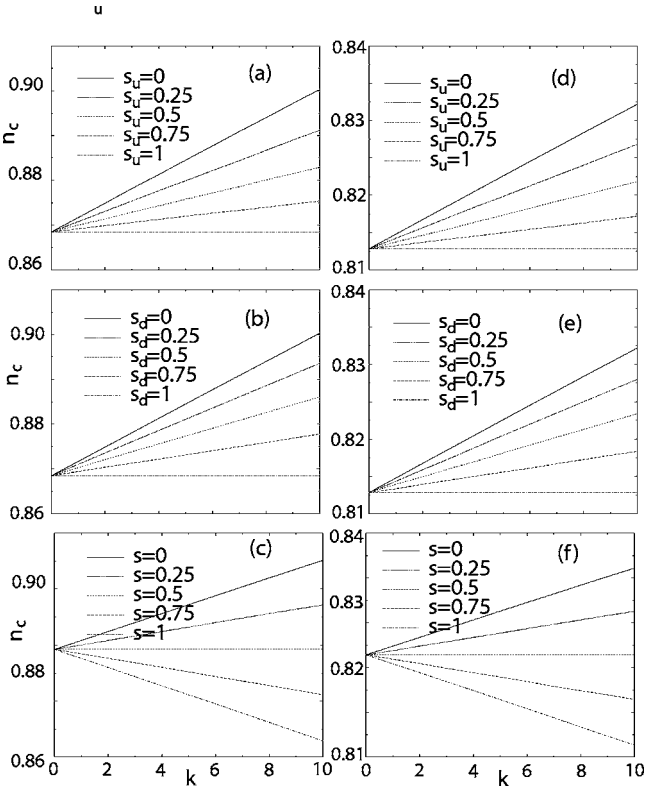

FIG. 4. The stability of hard-sphere fcc structures as functions of κ with $D=0.1$, $\ell=0.05$, $s_d=0$ in (a), $s_u=0$ in (b), and $s_u=s_d$ in (c). The corresponding values for the adhesive case (u_{sw} with $\beta A=1$ and $d=1.1$) are shown in (d)–(f).

critical density with adhesion than for the corresponding pure hard-sphere cases; reentrant transitions only occur when $d-1$ and A are small.

When we compare the results for the fcc crystal and for the glass, we see that generally increasing adhesion decreases the critical density. The change of the critical density for the glass is more substantial than the corresponding change for the stability limit of the fcc lattice. The width parameter d has a nonlinear effect on the critical density. The ability of d to change n_c decreases when d becomes larger, i.e., $\partial n_c/\partial d<0$ but $\partial^2 n_c/\partial d^2>0$.

B. Effects of motorization

When there is nonequilibrium kicking, generally, we must examine the critical density n_c as a function of the choice of $u_{st/sw}(r,A,d)$, temperature, uphill and downhill cooperative coefficient s_u and s_d, and relative strength of nonequilibrium effects expressed as a dimensionless ratio $\Delta := \kappa\ell^2/D$, i.e.,

$$n_c = n_c\left(\Delta, \frac{A}{k_BT}, d, u_{sw}/u_{st}\right). \tag{19}$$

As we previously estimated [14], based on practical values of cytoskeletal fibers, the range of Δ for the polymerization force alone can range from 10^{-3}–10^{-2} to above 1 for actin filaments.

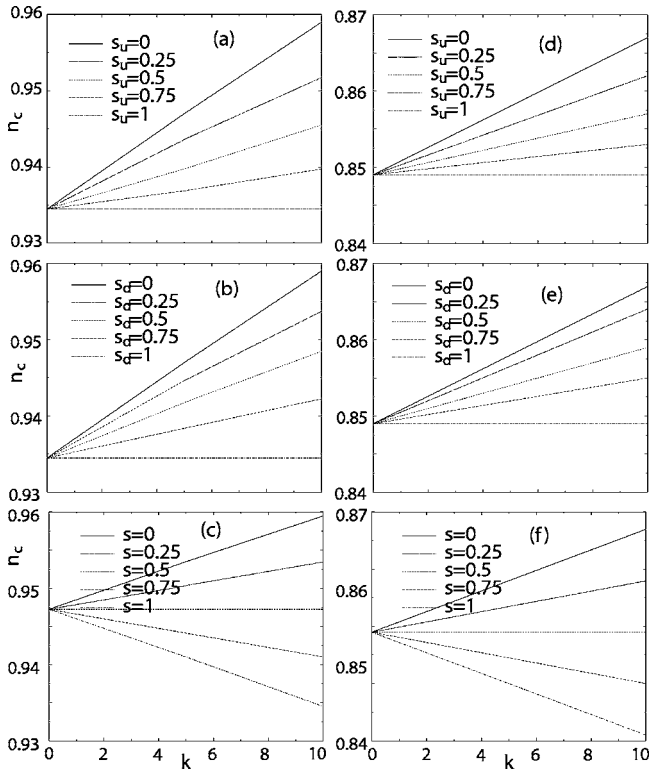

FIG. 5. The stability of hard-sphere glass as functions of κ with $D=0.1$, $\ell=0.05$, $s_d=0$ in (a), $s_u=0$ in (b), and $s_u=s_d$ in (c). The corresponding values for the adhesive case (u_{sw} with $\beta A=1$ and $d=1.1$) are shown in (d)–(f).

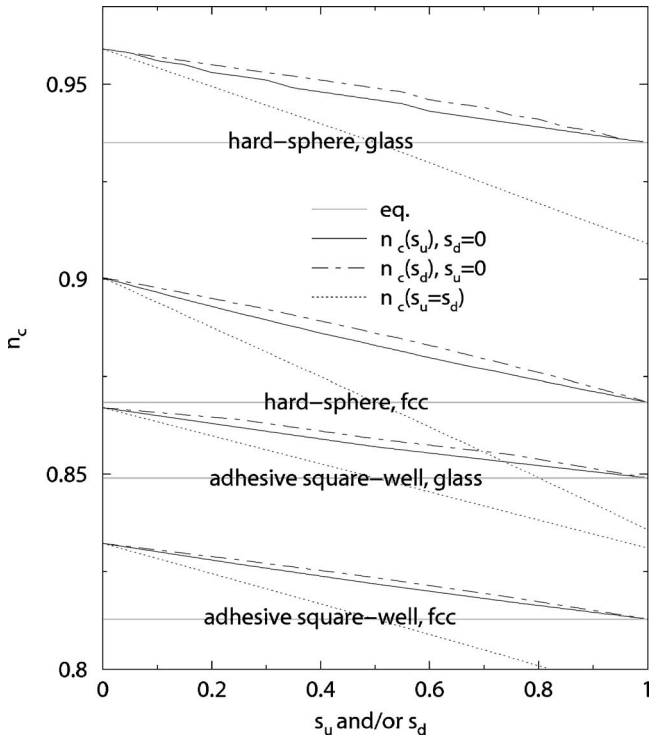

FIG. 6. The comparison of critical densities n_c of adhesive and pure hard spheres for the fcc lattice and glass. Four groups of critical densities are shown as functions of s_u and s_d at $\kappa=10$ and $\Delta=0.25$.

By comparing the results of the two variational methods we note that they give nearly the same results for critical densities when Δ is not very large. In fact, the error between them is less then 0.1% when $\Delta<1$. The corresponding phonon frequencies α and $\tilde{\alpha}$ also agree well with each other.

We first review the results for isotropic kicking. We show in the left panels of Fig. 4, for the cases of pure hard sphere on an fcc lattice, the critical density n_c as a function of κ at different values of the cooperative parameters s_u and s_d. We see the relation is quite linear, i.e., $\partial^2 n_c/\partial\kappa^2\approx 0$. The corresponding adhesive sphere cases are shown at the right panel of Fig. 4. We show in Fig. 5 the results for pure and adhesive hard-sphere glasses. Generally we see that the critical density grows with increasing reaction rate κ for low cooperative parameters $s_u+s_d<1$, while n_c actually decreases with increasing κ for $s_u+s_d>1$. We reorganize some of the data from Figs. 4 and 5 to show the results of n_c as a function of s at $\kappa=10$ in Fig. 6. A subtle feature from these plots is that $\partial^2 n_c/\partial s_u^2>0$ while $\partial^2 n_c/\partial s_d^2<0$. The range of changes with s for the fcc cases is larger than the corresponding ones of the glass cases.

We show the "effective" phonon frequencies α and $\tilde{\alpha}$ as functions of density n in Fig. 7 for the case of pure hard sphere and adhesive sphere fcc systems. We see that the difference between α and $\tilde{\alpha}$ increases with κ. For $\kappa>0$ and $s_u+s_d>1$ we have $\alpha>\tilde{\alpha}$ while for $\kappa>0$ and $s_u+s_d<1$, we have $\alpha<\tilde{\alpha}$.

For the persistent kicking cases, we show n_c as a function of the off center parameter b in Fig. 8. It turns out that b can quickly rise with Δ. Thus the range of b shown in Fig. 8 corresponds to small nonequilibrium kicking. We see four groups of lines corresponding to the pure hard spheres or adhesive spheres for the fcc or the glass cases. The upper and lower bounds correspond with the limiting cases $s=0$ and $s=1$, respectively. As expected, the critical density n_c generally decreases with increasing b.

V. CONCLUDING REMARKS

We have introduced a simple model of a collection of motorized particles and used this model to explore the effects of nonequilibrium energy pumping and equilibrium adhesion to the stability of systems made up of spherical particles.

Can we use these results to get an idea of how important nonequilibrium forces are in controlling the phases of the cytoskeleton? In the simple spherical model, we see that nonequilibrium motorization can have just as strong effects as does the binding of linker proteins represented as an adhesive energy term. For practical ratios of adhesive strength over the thermal energy and dimensionless nonequilibrium parameters A/k_BT and Δ, we find significant changes of the phase diagram. Thus both modulating adhesion and motorization can control cytoskeleton remodeling. Thus it is quite reasonable to stress that the nonequilibrium forces are important determinants of cellular mechanical properties. In our

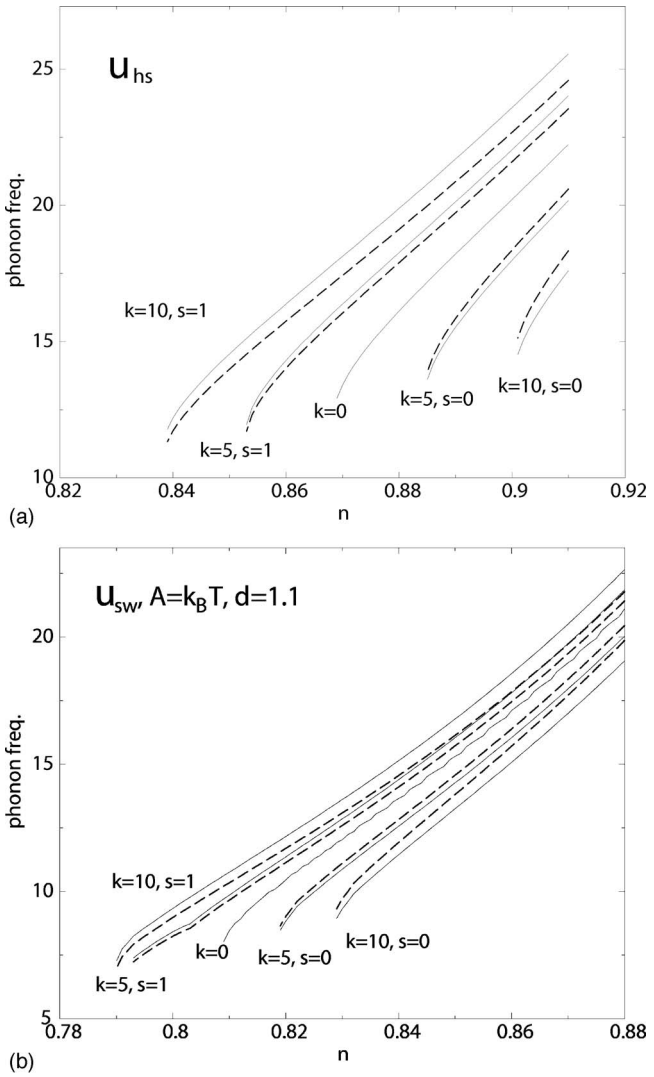

FIG. 7. Phonon frequencies α and/or $\tilde{\alpha}$ as a function of n for hard sphere and adhesive sphere fcc lattices with different parameters $\kappa=0,5,10$ and $s_u=s_d=0,1$. We set $\ell=0.05$ and $D=0.1$. The dashed lines are for $\alpha(n)$. The solid lines are for $\tilde{\alpha}(n)$. The two lines coincide at equilibrium case $\kappa=0$. For $\kappa>0$ and $s_u+s_d>1$, $\alpha>\tilde{\alpha}$ and vice versa.

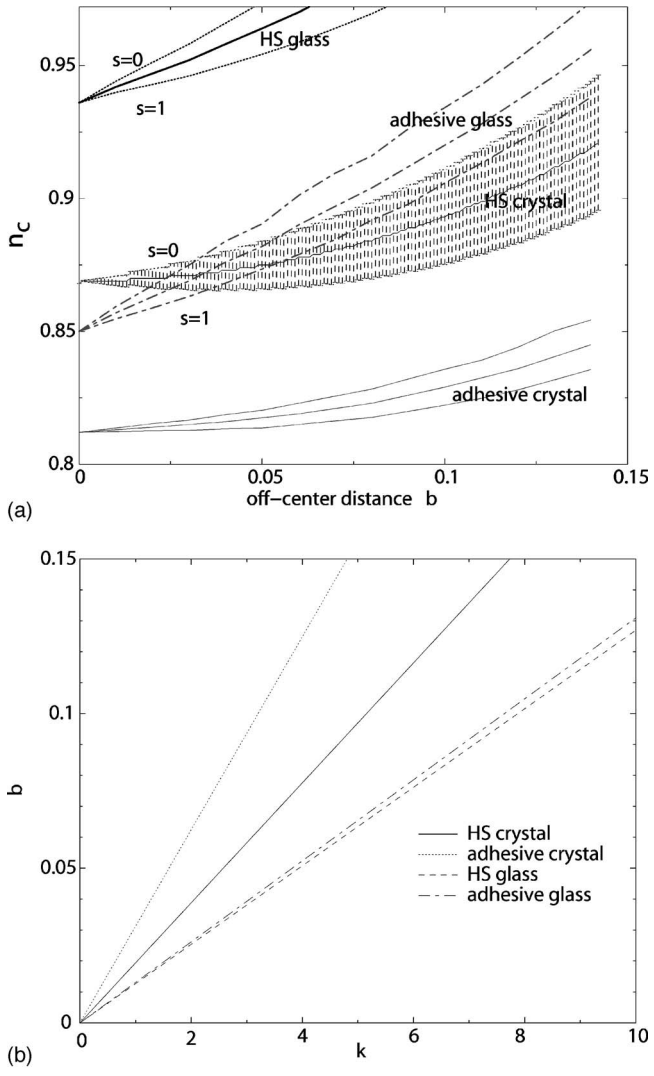

FIG. 8. The effect of the persistent kicking: the critical density as a function of the off-center parameter b. Four groups of plots are shown for glass and fcc, and for hard-sphere potential and adhesive hard-sphere potential cases. Here adhesive $u=u_{sw}(A=1,d=1.1)$.

view equilibrium colloidal models alone cannot completely explain the full story of cellular dynamics. The current model provides a basis that may be expanded to include more details relevant to specific experimental measurables [9] and to include architectural features of cell biology relevant to computational tensegrity models [37].

We see that nonequilibrium kicking and equilibrium responses together provide the tensions and compressions to maintain the cell shapes on the one hand, and fast remodeling when stimulated on the other hand. One important aspect of the tensegrity picture is the prestressed cytoskeleton. Thus it is tempting to calculate important macroscopic properties of assemblies such as the pressures and forces generated by such far-from-equilibrium matter. This calculation is not trivial. One certainly cannot use the usual route based on thermodynamic relations to relate phonon α and pressure as in [28]. Even what is meant by "pressure" might depend on how pressure is measured. One experimental setup will include direct construction of the interface between solid walls (or dead particles) and motorized particles. Such a problem belongs to a general important class of nonequilibrium interface problems which have interesting stability aspects, e.g., it may have exotic properties such as violations of the Gibbs phase rule [38]. We also note that steady states are only one possibility for statistical tensegrity models. More generally, one wonders whether the present model of the cytoskeleton can have macroscopic oscillations [39,40] under certain conditions. We hope to return to these issues in future works.

ACKNOWLEDGMENTS

We thank Dr. J. Ulander and Dr. R. W. Hall for very helpful discussions. This work is supported in part by NSF and CTBP.

[1] T. D. Pollard and W. C. Earnshaw, *Cell Biology* (W.B. Saunders, New York, 2002).
[2] D. Bray, *Cell Movements: From Molecules to Motility* (Garland Publishing, New York, 2001), 2nd ed.
[3] H. C. Berg, *Random Walks in Biology* (Princeton University Press, Princeton, 1993), 2nd ed.
[4] S. T. Wlodek, T. Shen, and J. A. McCammon, Biopolymers **53**, 265 (2000).
[5] G. M. Whitesides and B. Grzybowski, Science **295**, 2418 (2002).
[6] J. Howard, *Mechanics of Motor Proteins and the Cytoskeleton* (Sinauer Assoc., Sunderland, MA, 2001).
[7] S. J. Gunst and J. J. Fredberg, J. Appl. Physiol. **95**, 413 (2003).
[8] B. Fabry and J. J. Fredberg, Respir. Physiol. Neurobiol. **137**, 109 (2003).
[9] B. Fabry, G. N. Maksym, J. P. Butler, M. Glogauer, D. Navajas, and J. J. Fredberg, Phys. Rev. Lett. **87**, 148102 (2001).
[10] M. E. Chicurel, C. S. Chen, and D. E. Ingber, Curr. Opin. Cell Biol. **10**, 232 (1998).
[11] N. Wang, K. Naruse, D. Stamenovic, J. J. Fredberg, S. M. Mijailovich, I. M. Tolic-Norrelykke, T. Polte, R. Mannix, and D. E. Ingber, Proc. Natl. Acad. Sci. U.S.A. **98**, 7765 (2001).
[12] R. Connelly and A. Back, Am. Sci. **86**, 142 (1998).
[13] D. E. Ingber, J. Cell. Sci. **116**, 1157 (2003).
[14] T. Shen and P. G. Wolynes, Proc. Natl. Acad. Sci. U.S.A. **101**, 8547 (2004).
[15] L. A. Amos and W. B. Amos, *Molecules of the Cytoskeleton* (Guilford Press, New York, 1991).
[16] T. Loisel, R. Boujemaa, D. Pantaloni, and M.-F. Carlier, Nature (London) **401**, 613 (1999).
[17] S. Kuo and J. McGrath, Nature (London) **407**, 1026 (2000).
[18] T. Holy, M. Dogterom, B. Yurke, and S. Leibler, Proc. Natl. Acad. Sci. U.S.A. **94**, 6228 (1997).
[19] T. B. Liverpool and M. C. Marchetti, Phys. Rev. Lett. **90**, 138102 (2003).
[20] K. Kruse, J. F. Joanny, F. Julicher, J. Prost, and K. Sekimoto, Phys. Rev. Lett. **92**, 078101 (2004).
[21] D. F. Rosenbaum and C. F. Zukoski, J. Cryst. Growth **169**, 752 (1996).
[22] F. H. C. Crick and A. F. W. Hughes, Exp. Cell Res. **1**, 37 (1950).
[23] M. Dogterom and B. Yurke, Science **278**, 856 (1997).
[24] G. L. Eyink, Phys. Rev. E **54**, 3419 (1996).
[25] H. Chen, S. Chen, and R. H. Kraichnan, Phys. Rev. Lett. **63**, 2657 (1989).
[26] R. Jastrow, Phys. Rev. **98**, 1479 (1955).
[27] M. Fixman, J. Chem. Phys. **51**, 3270 (1969).
[28] J. Stoessel and P. G. Wolynes, J. Chem. Phys. **80**, 4502 (1984).
[29] H. Risken, *The Fokker-Planck Equation* (Springer, New York, 1996), 2nd ed..
[30] T. R. Koehler, Phys. Rev. Lett. **17**, 89 (1966).
[31] N. Werthamer, Phys. Rev. B **1**, 572 (1970).
[32] R. W. Hall and P. G. Wolynes, Phys. Rev. Lett. **90**, 085505 (2003).
[33] L. Verlet and J.-J. Weis, Phys. Rev. A **5**, 939 (1972).
[34] J. D. Weeks, D. Chandler, and H. C. Andersen, J. Chem. Phys. **54**, 5237 (1971).
[35] J. Bergenholtz and M. Fuchs, Phys. Rev. E **59**, 5706 (1999).
[36] K. N. Pham, A. M. Puertas, J. Bergenholtz, S. U. Egelhaaf, A. Moussad, P. N. Pusey, A. B. Schofield, M. E. Cates, M. Fuchs, and W. C. K. Poon, Science **296**, 104 (2002).
[37] C. Sultan, D. Stamenovic, and D. E. Ingber, Ann. Biomed. Eng. **32**, 520 (2004).
[38] G. Grinstein, IBM J. Res. Dev. **48**, 5 (2004).
[39] H. Fujita and S. Ishiwata, Biophys. J. **75**, 1439 (1998).
[40] F. Julicher, C. R. Acad. Sci., Ser IV: Phys., Astrophys. **2**, 849 (2001).